EURASIAN JOURNAL OF MATHEMATICAL AND COMPUTER APPLICATIONS
ISSN 2306–6172
Volume 12, Issue 2 (2024) 16 – 34

ON THE PROPERTIES OF A FAST ALGORITHM FOR SOLVING A THREE-DIMENSIONAL INVERSE PROBLEM OF SCALAR ACOUSTICS

Bakushinsky A.B., Leonov A.S.

Abstract The inverse single-frequency problem of scalar acoustics in three-dimensional space is considered. It consists in determining the characteristics of acoustic inhomogeneities lying in a flat layer from the distribution of the complex amplitude of the acoustic field in a flat recording layer. To effectively solve it, a special numerical algorithm is used, previously proposed and justified by the authors. As its component part, the algorithm uses solutions to special one-dimensional Fredholm equations of the 1st kind, and in the case of ambiguity in the solution of the latter, their normal solutions (solutions with a minimum norm) are sought. To regularize this ill-posed inverse problem, Tikhonov regularization and the TSVD method are used. A systematic numerical study is carried out of the influence of various parameters in the data recording scheme on the accuracy of the approximate solutions obtained using the algorithm. In particular, we study the dependence of this accuracy on the position of point sources and composite sources that cause sound vibrations, its dependence on the position of the data recording layer, and on the number of planes in which the recording sensors lie. It is shown that acceptable accuracy of approximate solutions can be obtained even with two such layers. In addition, an approach to the numerical study of the ambiguity of the solution to the inverse problem under consideration is proposed. It is based on special theoretical statements given in the article, and on the same numerical algorithm for solving the inverse problem. The approach is focused on comparing several normal solutions of one-dimensional integral equations from the problem under consideration. These normal solutions are calculated with respect to various elements. An example of using this theory to numerically estimate the non-uniqueness of a solution is given.

Key words: 3D scalar acoustics, inverse problem, regularization, solution error.

AMS Mathematics Subject Classification: 35R30.

DOI: 10.32523/2306-6172-2024-12-2-16-34

1 Introduction

This paper considers the inverse single-frequency problem of scalar acoustics. It is set for the following mathematical model. Let the function $p(\mathbf{x}, t)$, that depends on the coordinates $\mathbf{x} = (x, y, z)$ and time $t \geq 0$, determines the acoustic wave field in the medium, filling the space $\mathbb{R}^3$. The field is created by sources localized in the known region $S \subset \mathbb{R}^3$. The medium is characterized by a local phase speed of sound $c(\mathbf{x})$ and has a constant density. Moreover, it is known that $c(\mathbf{x}) = c_0 = \text{const}$ outside the given region $X \subset \mathbb{R}^3$ satisfying the condition $X \cap S = \emptyset$. In the region X itself, the function $c(\mathbf{x})$ can be variable, and this is interpreted as the presence of acoustic

inhomogeneities there. Then, for a harmonic source of oscillations of the form $f(\mathbf{x})e^{i\omega t}$ with a known frequency ω, the field $p(\mathbf{x},t)$ within the framework of the linear acoustics approximation can be found in the form $p(\mathbf{x},t) = u(\mathbf{x},\omega)e^{i\omega t}$. The complex amplitude $u(\mathbf{x},\omega)$ of this field, depending on frequency as a parameter, satisfies the equation

$$\Delta u(\mathbf{x},\omega) + k_0^2 u(\mathbf{x},\omega) = f(\mathbf{x}) + \omega^2 \xi(\mathbf{x}) u(\mathbf{x},\omega),\ \mathbf{x} \in \mathbb{R}^3, \tag{1}$$

and radiation condition (see, for example, [15]). Here $k_0 = \frac{\omega}{c_0}$ and $\xi(\mathbf{x}) = c_0^{-2} - c^{-2}(\mathbf{x})$.

We are interested in the following *inverse problem* for the equation (1): knowing for a given frequency (or frequencies) ω the complex amplitude of the field $u(\mathbf{x},\omega)$ in the region $Y,\ Y \cap X = \emptyset, Y \cap S = \emptyset$, find the coefficient $\xi(\mathbf{x})$, i.e. as a result, the function $c(\mathbf{x})$, which determines the acoustic inhomogeneities in the region X.

Problems of this kind have been studied in numerous works (see, for example, [6, 10, 15, 16, 22, 24], etc.) from both theoretical and applied points of view. In particular, the question of an effective numerical algorithm for solving them was also considered [1, 2, 6, 7, 8, 9, 13, 14, 17, 18, 19, 23]. It turned out that approximate solution of a three-dimensional inverse problem using standard methods on sufficiently detailed grids "in a reasonable time" (tens of minutes) requires significant computing resources (computing clusters, supercomputers) [1, 2, 13, 14, 7, 23, 6]. On the other hand, the average researcher usually has access to only personal computers (PCs) of average performance, and would like to somehow solve such inverse problems on a PC. In this regard, in the series of works [3, 4, 5] we proposed an approach that allows us to develop time-efficient algorithms for solving such three-dimensional inverse problems. The approach is as follows.

By introducing the Green's function for the Helmholtz equation (1) in $\mathbb{R}^3$:

$$G(r,\omega) = -\frac{\exp(i\omega r/c_0)}{4\pi r},\ r = |\mathbf{x}| = \sqrt{x^2+y^2+z^2}, \tag{2}$$

it is possible, under certain assumptions about the smoothness of the functions $u(\mathbf{x},\omega)$, $f(\mathbf{x})$, $c(\mathbf{x})$ (see, for example, [1, 2, 10, 13, 15, 24]) reduce the main inverse problem to a nonlinear system of integral equations for unknowns $u(\mathbf{x}',\omega),\ \xi(\mathbf{x}'),\ \mathbf{x}' \in X$:

$$\begin{aligned} u(\mathbf{x},\omega) = u_0(\mathbf{x},\omega) + \omega^2 \int_X G(|\mathbf{x}-\mathbf{x}'|,\omega)\xi(\mathbf{x}')u(\mathbf{x}',\omega)d\mathbf{x}',\ \mathbf{x} \in X, \\ \omega^2 \int_X G(|\mathbf{x}-\mathbf{x}'|,\omega)\xi(\mathbf{x}')u(\mathbf{x}',\omega)d\mathbf{x}' = W(\mathbf{x},\omega),\ \mathbf{x} \in Y. \end{aligned} \tag{3}$$

The functions included here, namely

$$u_0(\mathbf{x},\omega) = \int_X G(|\mathbf{x}-\mathbf{x}'|,\omega)f(\mathbf{x}')d\mathbf{x}',\ \ W(\mathbf{x},\omega) = u(\mathbf{x},\omega) - u_0(\mathbf{x},\omega),\ \ \mathbf{x} \in Y,$$

are known or computable, and the quantities $u(\mathbf{x},\omega)$, $\xi(\mathbf{x})$, $\mathbf{x} \in X$, are to be determined from nonlinear system of equations (3). The latter can be reduced to the following sequence of linear problems.

1) Solve the second equation, written in the form

$$\int_X G(|\mathbf{x}-\mathbf{x}'|,\omega)v(\mathbf{x}',\omega)d\mathbf{x}' = w(\mathbf{x},\omega),\ \ \mathbf{x} \in Y, \tag{4}$$

with respect to the function $v(\mathbf{x}',\omega)=\xi(\mathbf{x}')u(\mathbf{x}',\omega),\ \mathbf{x}'\in X$. Here $w(\mathbf{x},\omega)=\frac{W(\mathbf{x},\omega)}{\omega^2}$.
2) Calculate the function $u(\mathbf{x},\omega),\ \mathbf{x}\in X$, from the first equality of the system (3) written in the form

$$u(\mathbf{x},\omega)=u_0(\mathbf{x},\omega)+\omega^2\int_X G(|\mathbf{x}-\mathbf{x}'|,\omega)v(\mathbf{x}',\omega)d\mathbf{x}',\ \mathbf{x}\in X. \tag{5}$$

3) Find the function $\xi(\mathbf{x})$ from the equation $v(\mathbf{x},\omega)=\xi(\mathbf{x})u(\mathbf{x},\omega),\ \mathbf{x}\in X$.

A similar procedure was used previously (see, for example, [12]). However, besides this, we use additional information about the form of the regions X, Y, considering them to be flat parallel infinite layers of finite thickness. Then, using two-dimensional Fourier transforms, it is possible to significantly simplify procedure 1 - 3, reducing three-dimensional integral equations (4) to a set of one-dimensional integral equations, and the problem (5) can be represented as calculating a series of one-dimensional integrals. The details of this approach and the exact formulations will be outlined below. The result is a speed-efficient method (algorithm) for solving the inverse problem with data in a flat layer. A similar approach was used in the work [5] for cylindrical layers.

In the works [3, 4, 5] we paid main attention to studying the speed of the proposed method (algorithm) for solving the inverse problem. At the same time, some other properties of this method remained unexplored, and in this work we will address this issue. The main attention will be paid to clarifying the influence of changes in the set of input data of the inverse problem (the number and positions of sources, the structure of the data recording layer, etc.) on the "quality" of the resulting solution. Along the way, we will discuss the problem of uniqueness (non-uniqueness) of the solution obtained using our algorithm, drawing attention to the fact that the phrase "uniqueness of the solution" makes sense only if the set of elements to which the desired solution belongs is indicated.

We assume that in problem (1), i.e. in formulas (4), (5), only one frequency is used. This is done in order to more clearly highlight the influence of changes in the spatial data of the inverse problem on the solution obtained using the algorithm. Accordingly, for brevity we will omit the symbol ω when writing the arguments of the functions $G(|\mathbf{x}|,\omega)$, $u(\mathbf{x},\omega)$, etc. Note that the algorithm for solving the inverse problem at several frequencies was tested earlier in the works [4, 5].

The presentation is structured as follows. In Sect.2 we give a description of algorithms for solving the considered direct and inverse problems. Next, Sect.3 provides a description of the main model inverse problem on which the algorithm is tested. Sect.4 studies the influence of the position of a point source on the accuracy of the found approximate solution. Sect.5 examines the influence of the position of the composite source on the accuracy of the calculated solution and compares various regularizing algorithms (RAs) used for calculations. The effect of the number of data sensors (i.e., grid sizes in the observation area) on the solution accuracy is studied in Sect.6. Sect.7 considers the problem of uniqueness/non-uniqueness of a solution to the inverse problem under study and contains some statements that are further used in Sect.8 to explore numerically the non-uniqueness of a solution in the model example under consideration. Sect.9 contains brief conclusions from the work.

2 Description of algorithms for solving direct and inverse problems

We assume that the regions X, Y introduced above are flat layers of the form

$$X = \mathbb{R}^2_{xy} \times [z_1, z_2],\ Y = \mathbb{R}^2_{xy} \times [z_3, z_4].$$

Suppose that the function $\xi(\mathbf{x})$ is finite in X. We use the two-dimensional Fourier transform in variables (x, y), which is calculated for the function $a(\mathbf{x}) = a(x, y, z) \in L_2(\mathbb{R}^2_{xy})$ with fixed z:

$$\tilde{A}(z, \Omega) = F_{xy}\left[a(\mathbf{x})\right](\Omega) = \int\limits_{\mathbb{R}^2_{xy}} a(x, y, z) \exp\left(i(\Omega_1 x + \Omega_1 y)\right) dxdy, \quad \Omega = (\Omega_1, \Omega_2) \in \mathbb{R}^2,$$

as well as the inverse Fourier transform $F^{-1}_{\Omega}\left[\tilde{A}(z, \Omega)\right](x, y)$. One can verify that for the Green's function (2) such Fourier transform, $\tilde{G}(z, \Omega)$, exists. Let us assume that inclusions $u(\mathbf{x}), u_0(\mathbf{x}) \in L_2(X)$, $w(\mathbf{x}) \in L_2(Y)$ take place. Then the existence of Fourier images

$$\tilde{U}(z, \Omega), \tilde{U}_0(z, \Omega),\ z \in [z_1, z_2],\ \ \tilde{W}(z, \Omega),\ z \in [z_3, z_4],$$

of these functions is ensured, respectively. Let us also take into account that the Fourier image $\tilde{V}(z, \Omega)$, $z \in [z_1, z_2]$, of the function $v(\mathbf{x}) = \xi(\mathbf{x})u(\mathbf{x})$ exists due to the finiteness of $\xi(\mathbf{x})$. Next, transforming the integrals from formulas (4), (5), we obtain

$$\int_{z_1}^{z_2} \tilde{G}(z - z', \Omega)\tilde{V}(z', \Omega)dz' = \tilde{W}(z, \Omega), \quad z \in [z_3, z_4];$$

$$\tilde{V}(z', \Omega) = F_{xy}\left[\xi(x, y, z')F^{-1}_{\Omega}\left[\tilde{U}(z', \Omega)\right](x, y)\right](\Omega), \ \ z' \in [z_1, z_2];$$

$$\tilde{U}(z, \Omega) = \tilde{U}_0(z, \Omega) + \omega^2 \int_{z_1}^{z_2} \tilde{G}(z - z', \Omega)\tilde{V}(z', \Omega)dz', \ \ z \in [z_1, z_2]. \quad (6)$$

We will use these equalities to solve the direct and inverse problems. Let us formulate the corresponding algorithms.

2.1 Solving the direct problem.

The direct problem for the equalities (4), (5) is to find the function $w(\mathbf{x})$, $\mathbf{x} \in Y$, using the given functions $u_0(\mathbf{x})$ and $\xi(\mathbf{x})$. For Fourier images, this corresponds by virtue of (6) to finding the function $\tilde{W}(z, \Omega)$ of the argument $z \in [z_3, z_4]$ for each parameter Ω, using the function $\xi(x, y, z)$, $z \in [z_1, z_2]$, and the function $\tilde{U}_0(z, \Omega)$ of the argument $z \in [z_1, z_2]$ given (computed) for these parameters. The solution is carried out as follows.

Algorithm 1.

1) Calculate the Fourier transform $\tilde{U}_0(z, \Omega)$. In practice, this is implemented using the fast discrete Fourier transform (FFT).

2) Set the iterative process

$$\tilde{U}_{n+1}(z,\Omega) = \tilde{U}_0(z,\Omega) + \omega^2 \int_{z_1}^{z_2} \tilde{G}(z-z',\Omega)\tilde{V}_n(z',\Omega)dz', \quad z \in [z_1,z_2],$$
$$\tilde{V}_n(z',\Omega) = F_{xy}\left[\xi(x,y,z')F_\Omega^{-1}\left[\tilde{U}_n(z',\Omega)\right](r)\right](\Omega), \quad z' \in [z_1,z_2], \ n = 0,1,... \quad (7)$$

starting with the function $\tilde{U}_0(z,\Omega)$.
3) Stop the process according to some rule at the iteration with $n = \nu - 1$ and obtain an approximate solution $\tilde{U}_\nu(z,\Omega)$ of the first equation in the group (7).
4) Calculate sequentially the quantities

$$\tilde{V}_\nu(z',\Omega) = F_{xy}\left[\xi(x,y,z')F_\Omega^{-1}\left[\tilde{U}_\nu(z',\Omega)\right](r)\right](\Omega), \quad z' \in [z_1,z_2],$$
$$\tilde{W}_\nu(z,\Omega) = \int_{z_1}^{z_2} \tilde{G}(z-z',\Omega)\tilde{V}_\nu(z',\Omega)dz', \quad z \in [z_3,z_4] \quad (8)$$

and accept the function $\tilde{W}_\nu(z,\Omega)$ and its inverse Fourier transform as an approximate solution to the direct problem.

We use Algorithm 1 only to generate model data for the inverse problem. The analysis of its convergence (at least for "small" ω) is briefly discussed in the work [4].

2.2 Solving the inverse problem.

The inverse problem consists of finding the function $\xi(x,y,z)$, $z \in [z_1,z_2]$, from the system (6) using the value $\tilde{W}(z,\Omega)$, $z \in [z_3,z_4]$, specified for each parameter Ω. This is done in the following algorithm.

Algorithm 2.

1) Using the given function $\tilde{W}(z,\Omega) \in L_2$ we solve one-dimensional integral equations of the 1st kind

$$\int_{z_1}^{z_2} \tilde{G}(z-z',\Omega)\tilde{V}(z',\Omega)dz' = \tilde{W}(z,\Omega), \quad z \in [z_3,z_4] \ \Rightarrow \tilde{V}(z',\Omega) \in L_2, \quad (9)$$

for each parameter Ω. Here we apply an appropriate method for regularizing these, generally speaking, ill-posed problems.
2) Using the found function $\tilde{V}(z',\Omega)$ we calculate the value

$$\tilde{U}(z,\Omega) = \tilde{U}_0(z,\Omega) + \omega^2 \int_{z_1}^{z_2} \tilde{G}(z-z',\Omega)\tilde{V}(z',\Omega)dz', \quad z \in [z_1,z_2], \quad (10)$$

and then find the functions

$$V(x,y,z) = F_\Omega^{-1}\left[\tilde{V}(z,\Omega)\right](x,y), \quad u(x,y,z) = F_\Omega^{-1}\left[\tilde{U}(z,\Omega)\right](x,y), \quad (x,y,z) \in X.$$

In practice, this is done using inverse FFT.
3) We find the function $\xi(x,y,z)$ from the equation $u(x,y,z)\xi(x,y,z) = V(x,y,z)$. This can be done using the least squares method (LSM) or simply computing the

solution as $\xi(x,y,z) = V(x,y,z)/u(x,y,z)$. Generally speaking, the result depends on the frequency ω.

The issues of numerical implementation of this algorithm are considered in detail in the works [3, 4, 5]. Its high speed, achieved through the use of FFT, was also confirmed there. Here we will numerically explore other properties of Algorithm 2.

3 Description of the main model problem

In this work, we studied Algorithm 2 for a number of model problems with various solutions in the form of local acoustic inhomogeneities (finitely supported functions $\xi(\mathbf{x})$ with relatively small carrier sizes). For definiteness, below we present the results of solutions for only one typical model inverse problem in dimensionless variables. It is supposed everywhere that $c_0 = 1$ и что $k_0 = \omega = 3$. In the area of solutions,

$$X = [-7,7] \times [-7,7] \times [-1,1.5] = \Pi_{xy} \times [z_1, z_2],$$

uniform grids of size $N \times N \times M$ with $N = 128$, $M = 51$ were used for variables x, y, z. In the observation area represented by the "thin layer"

$$Y = [-7.7] \times [-7.7] \times [z_3, z_3 + 0.1] = \Pi_{xy} \times [z_3, z_3 + 0.1]$$

uniform grids of size $N \times N \times M_1$ for variables x, y, z' were also used with $N = 128$ and different $M_1, M_1 = 2, 4, 8$. Model sources were specified in the form

$$f(\mathbf{x}) = \sum_m \delta(\mathbf{x} - \mathbf{x}_m),$$

where $\mathbf{x}_m$ are the coordinates of δ-shaped point sources. The exact solution is expressed as $\bar{\xi}(x,y,z) = \bar{\xi}_1(x,y,z) + \bar{\xi}_2(x,y,z)$. Its terms have supports $X_1 = \{D_1(x,y,z) \leq D_2(x,y,z)\}$ and $X_2 = \{D_3(x,y,z) \leq 0.01\}$ respectively, where

$$D_1(x,y,z) = \left((x-1)^2 + (y+2)^2 + (z-0.5)^2 + R^2 - r^2\right)^2,$$
$$D_2(x,y,z) = 4R^2\left((x-1)^2 + (y+2)^2\right),$$
$$D_3(x,y,z) = (x+3)^2 + (y-2)^2 - (x+3)(z-0.5) + (z-0.5)^2,$$

and $R = 0.7, r = 0.2$. The terms themselves have the form

$$\bar{\xi}_1(x,y,z) = \exp\left[200\left(D_1(x,y,z) - D_2(x,y,z)\right)\right], \bar{\xi}_2(x,y,z) = 0.5\exp\left[-200 D_3(x,y,z)\right].$$

Geometrically, the exact solution of the inverse problem is defined on carriers in the form of a torus and an ellipsoid with the distribution of the quantities $\bar{\xi}_{1,2}(\mathbf{x})$ in them in the form of Gaussians, rapidly decreasing from the boundaries to the centers of carriers. Model data for solving the inverse problem were calculated using Algorithm 1 with the source functions $f(\mathbf{x})$ and the model solution $\bar{\xi}(\mathbf{x})$. These data were used in unperturbed form when solving the inverse problem in order to see (in a pure form) the influence of their changes on approximate solutions for various source positions and observation areas. Studies of the effect of random data perturbations on solutions to the inverse problem were previously carried out in the works [3, 4, 5] and are not considered here. The support of exact model solution to the inverse problem, as well as numbered possible positions of point sources and the position of one of the planes in the observation area, are shown in Fig.1.

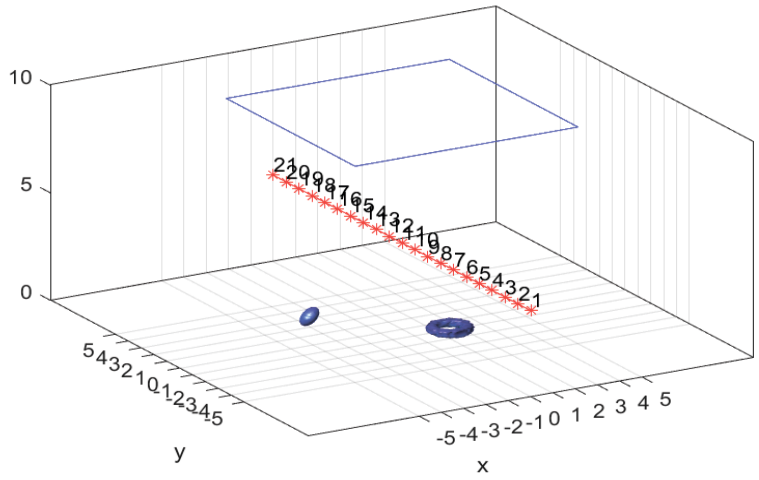

Figure 1: The exact solution support (ellipsoid and torus), point source line, source positions (asterisks), their numbers, and one of the planes in the observation area (rectangle) are depicted.

4 The influence of the position of a point source on the accuracy of calculated solution

In this section, we study two questions using numerical experiments.

1) Given a "thin layer" of observation, what position of one δ-shaped source gives the smallest error in the approximate solution?

2) Given the position of the source, which observation layer is better to take: close to the observation area or far away, so that the algorithm error is minimal?

Thus, to answer the second question, we will optimize the "height" of the observation layer z_3, and to answer the first, we will optimize the position of one point source on various straight lines like the one shown in Fig.1.

The following estimate of the relative error of the approximate solution $\tilde{\xi}(\mathbf{x})$ is taken as an optimality criterion :

$$\Delta = \max \left\{ \frac{\left\| \tilde{\xi}(x,y,z) - \bar{\xi}(x,y,z) \right\|_{L_2(\Pi_{xy})}}{\left\| \bar{\xi}(x,y,z) \right\|_{L_2(\Pi_{xy})}} : \ z \in [z_{\min}, z_{\max}] \right\}. \tag{11}$$

Here $\bar{\xi}(x,y,z)$ and $\tilde{\xi}(x,y,z)$ are an exact (model) solution and some approximate solution of the inverse problem. This criterion was chosen due to the specifics of Algorithm 2. In it, for each point $(x,y) \in \Pi_{xy}$ the solutions are found as functions of the argument z. Thus, the error estimate (11) means first calculating the average error

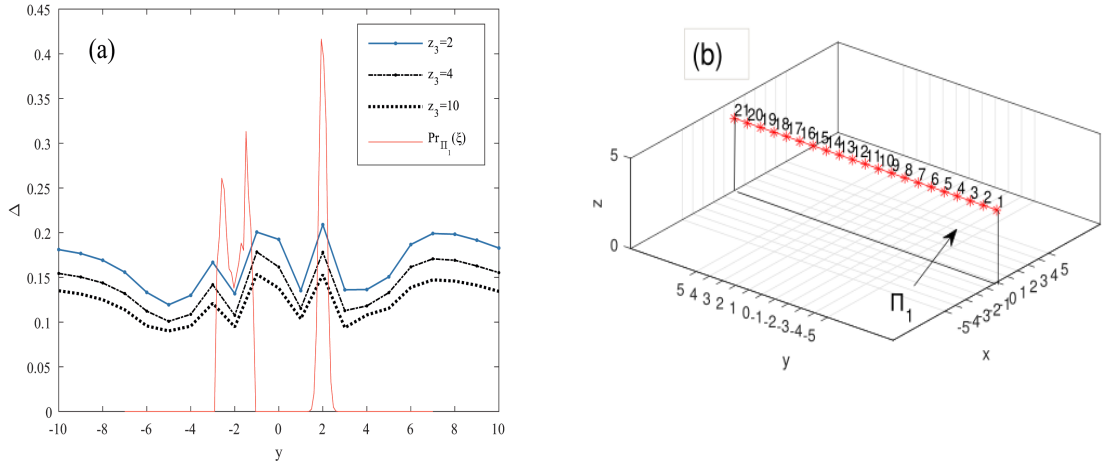

Figure 2: (a) Error Δ as a function of the position y of a point source on line ℓ_1 (for three positions of the observation layer z_3). The solid line marks the projection of the exact solution onto the source plane Π_1. (b) The best solution found for various positions of a point source on line ℓ_1 for the observation layer $z_3 = 4$.

over the points $(x, y) \in \Pi_{xy}$:

$$\Delta_0(z) = \frac{\left\| \tilde{\xi}(x,y,z) - \bar{\xi}(x,y,z) \right\|_{L_2(\Pi_{xy})}}{\left\| \bar{\xi}(x,y,z) \right\|_{L_2(\Pi_{xy})}}, \tag{12}$$

for each admissible fixed z, and then calculating the maximum error over all depths z.

When studying the first question, it was assumed that the source can occupy fixed positions on the lines $\ell_1 - \ell_4$ shown in Fig.2–5. The inverse problem was solved for each such source position, for three heights z_3: $z_3 = 2$, 4, 10, of the observation layer, and the corresponding error Δ was calculated. The results obtained, i.e. dependence of the error Δ on the positions of the point source, and the best of all approximate solutions found for various positions of a point source on the corresponding straight line ℓ, are presented in Fig.2–5. Three-dimensional images of the approximate solution are presented in the form of surfaces bounding the carrier. Due to the large amount of graphic material, this is done only for one of the heights z_3 of the data layer.

Analysis of these results leads to the following intermediate conclusions.

a) The error Δ depends significantly on both the position of the point source and the position of the observation layer. This error can range from $5 - 8\%$. An "unsuccessful" line for source positions can spoil the quality of the approximate solution (see Fig.4).

b) With increasing z_3, i.e. when the observation layer is distanced from acoustic inhomogeneities, the accuracy improves for all source positions. However, experiments have shown that it practically stops changing at $z_3 > 10$. In addition, for large z_3, artifacts sometimes appear in the approximate solution, namely, false solutions on deep z-layers of the solution (see, for example, Fig.3).

c) The error is significantly reduced (by $4\% - 8\%$), if the point source turns out to be "to the side" of the projection of the exact solution onto the plane of sources Π_1.

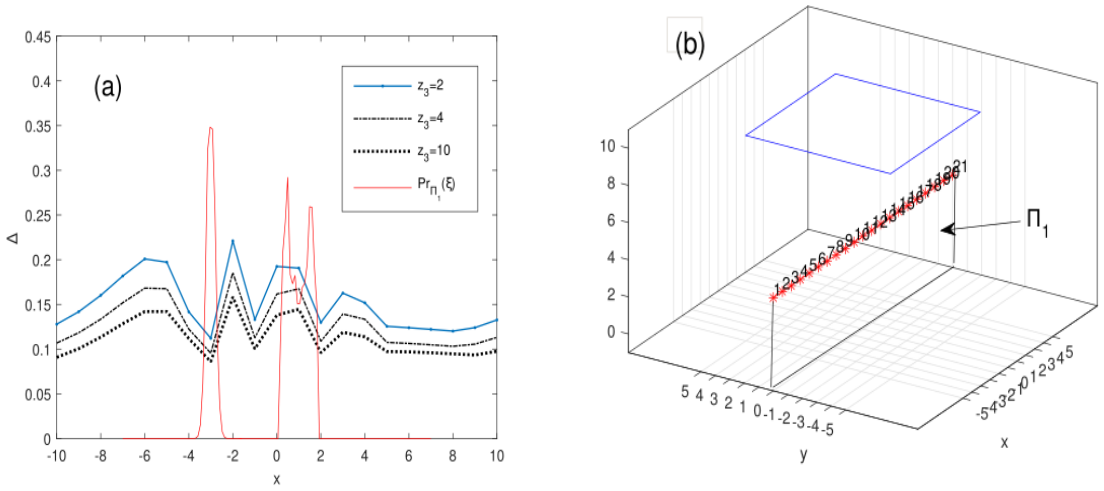

Figure 3: (a) Error Δ as a function of the position of a point source on the line ℓ_2. (b) The best solution found for various positions of a point source on line ℓ_2 for the observation layer $z_3 = 10$.

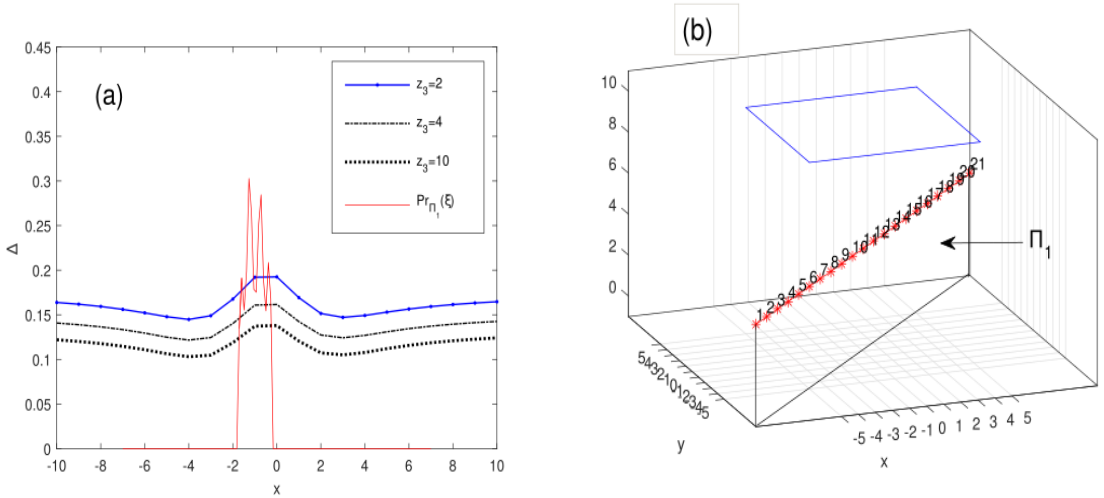

Figure 4: (a) Error Δ as a function of the position of a point source on the line ℓ_3. (b) The best solution found for various positions of a point source on line ℓ_3 for the observation layer $z_3 = 10$.

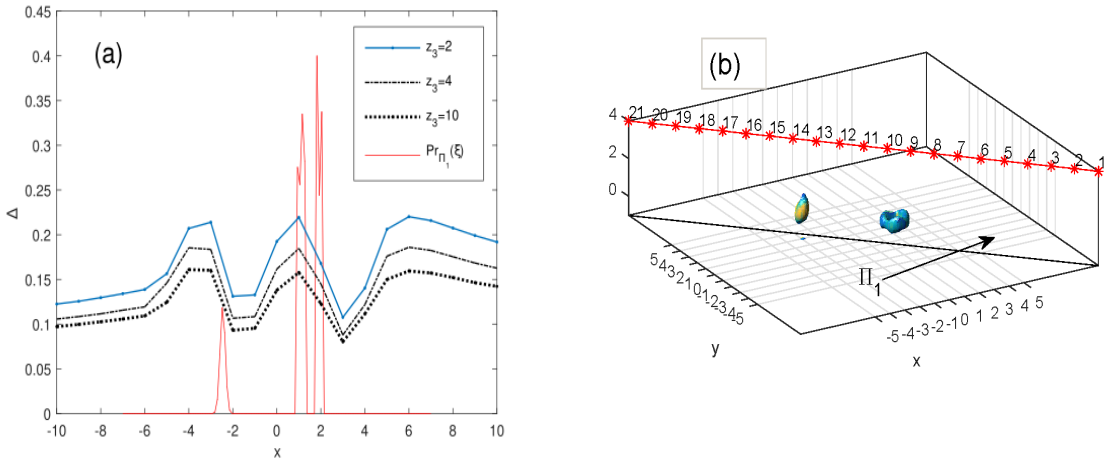

Figure 5: (a) Error Δ as a function of the position of a point source on the line ℓ_4. (b) The best solution found for various positions of a point source on line ℓ_4 for the observation layer $z_3 = 4$.

Thus, it is better to use Algorithm 2 with a point source located not directly above the acoustic inhomogeneities but at some, not very large, angle to them.

5 The influence of the position of the composite source on the accuracy of the solution

In the next series of experiments, a composite source was used, namely: a set of 21 point sources lying on lines of the ℓ type (see, for example, Fig.1). The main question that was studied is formulated as follows: what line of sources ℓ and what position of the data recording layer z_3 should be taken in order to minimize the solution error of the form (12), $\Delta_0(z)$, that is, the average error of the solution section at the depth z. Two methods for solving one-dimensional integral equations were compared at step 1 of algorithm 2: the A.N. Tikhonov regularization method (TRA) of zero order (see [25]) and the TSVD algorithm (see, e.g. [11]) with regularization parameters found by the V.A. Morozov discrepancy principle [21]. We present the results obtained in Fig.6–9.

Analyzing these results, the following conclusions can be drawn. i) In general, the error of the TRA method is comparable to the error of the TSVD method. Sometimes, it turns out to be somewhat smaller for the depths z at which heterogeneities occur ($0 \le z \le 1$). For this reason, we will further present only the results of calculations using the TRA method. ii) The errors of both methods increase significantly with increasing depth of the study ($z < 0$). iii) The smallest maximum errors are obtained for sources lying on ℓ_4 line, which is closest to the inhomogeneities.

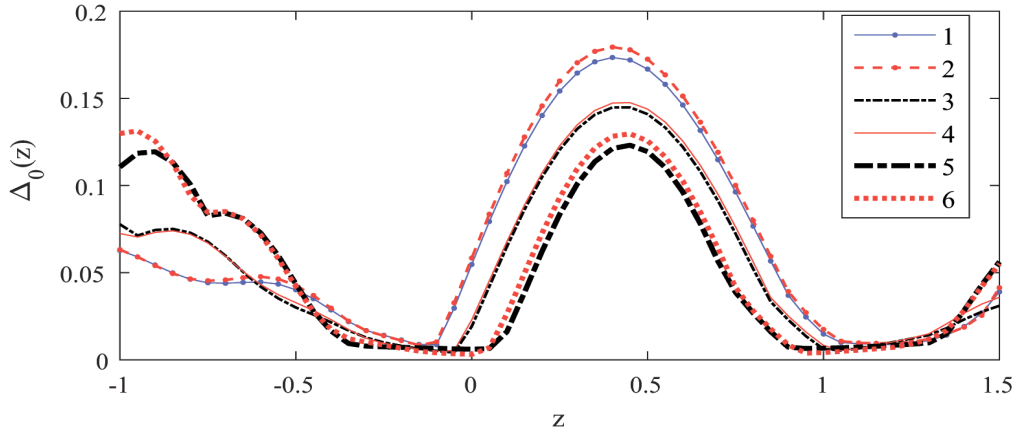

Figure 6: Composite source on line ℓ_1. Comparison of TRA and TSVD in terms of accuracy $\Delta_0(z)$ for different z_3. Curves 1,3,5 are the zero-order Tikhonov RA accuracies for $z_3 =$ 2, 4, 10 respectively. Curves 2,4,6 are similar lines for TSVD.

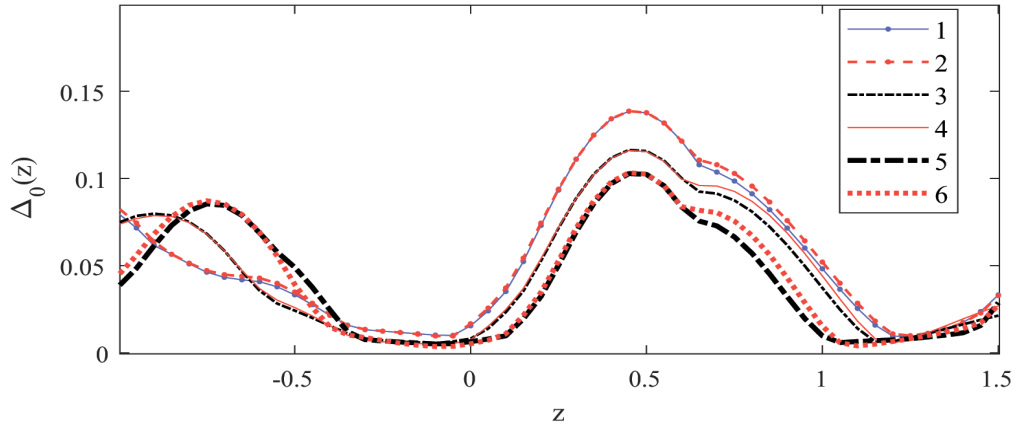

Figure 7: The same for the composite source on the line ℓ_2.

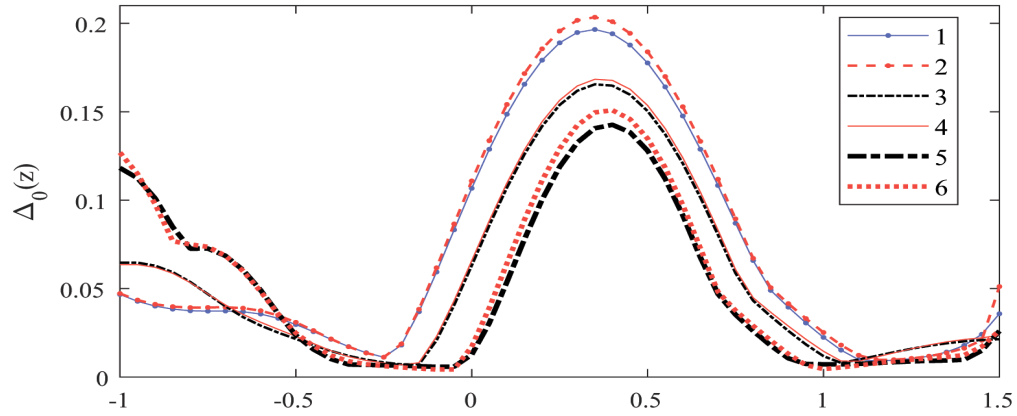

Figure 8: The same for the composite source on the line ℓ_3.

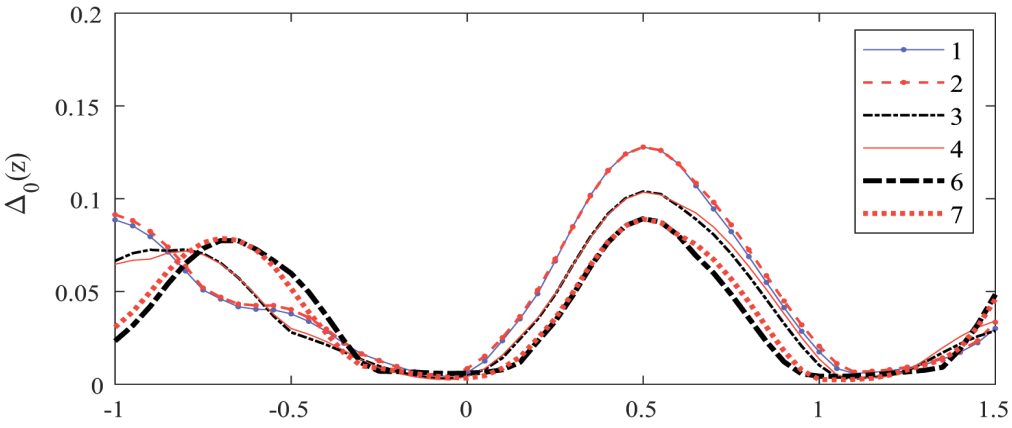

Figure 9: The same for the composite source on the line ℓ_4.

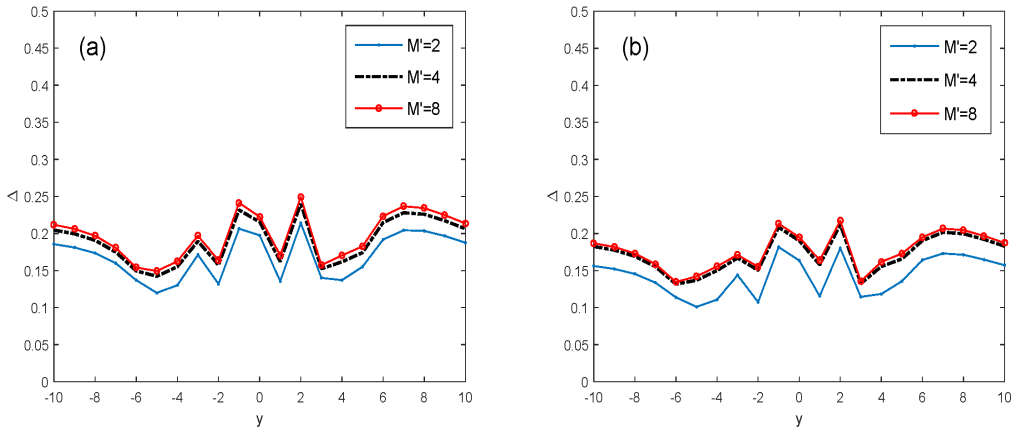

Figure 10: (a) Error Δ as a function of the position of point source y on line ℓ_1 for the observation layer $z_3 = 2$ and a different number M' of sensor layers. (b) The same for the observation layer $z_3 = 4$.

6 The influence of the number of data sensors on the accuracy of the solution

The accuracy of Algorithm 2 was also studied depending on the number of planes of the form $z = \text{const}$ lying in the layer $Y = [-7, 7] \times [-7, 7] \times [z_3, z_3 + 0.1]$, in which the data of the inverse problem are measured. The study was carried out for layers with different heights z_3. These planes model sets of sensors located within the observation layer. The study also considers different positions of a point source on two lines ℓ_1, ℓ_4. The accuracy of Algorithm 2, depending on the ordinate y of the point source on the corresponding line, is determined by the formula (11). The results are presented in Fig.10, 11.

It can be seen that two layers of sensors provide better accuracy to the algorithm than more. At $M' \geq 4$ the value of Δ stops changing, and the accuracy of the algorithm saturates. This is true for all considered heights z_3 of the observation layer.

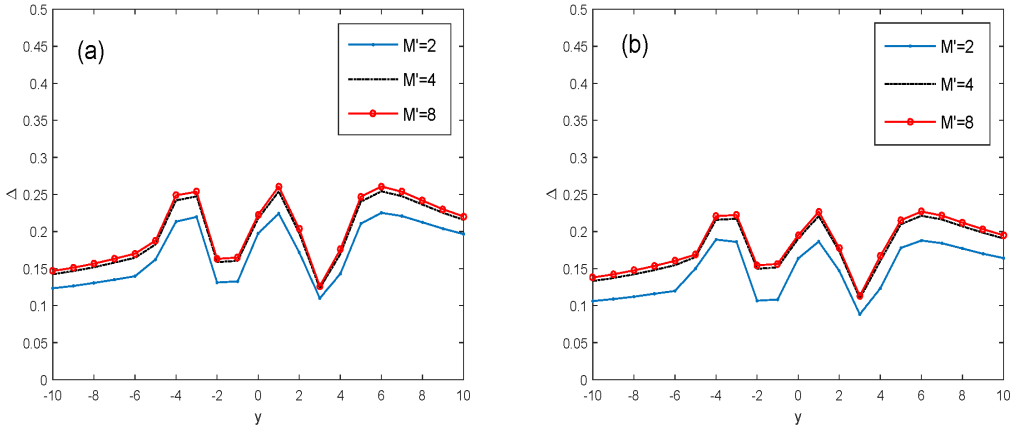

Figure 11: (a) Error Δ as a function of source position y on line ℓ_4 for observation layer $z_3 = 2$ and varying number M' of sensor layers. (b) The same for the observation layer $z_3 = 4$.

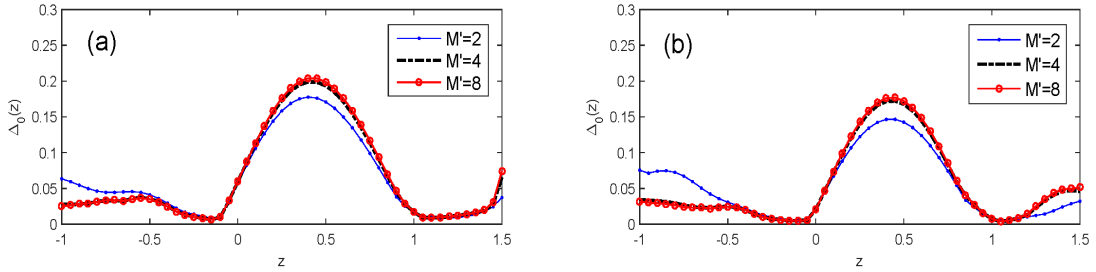

Figure 12: Composite source on ℓ_1. (a) Comparison of the accuracy $\Delta_0(z)$ of the algorithm for $z_3 = 2$ and for different numbers M' of sensor layers. (b) The same for $z_3 = 4$.

A similar study for various positions of a linear (composite) source was carried out for two lines ℓ_1, ℓ_4 filled with point sources. The accuracy of Algorithm 2 is defined here by the formula (12). The results are given in Fig.12, 13.

As in the case of a point source, two layers of sensors provide better accuracy of the algorithm at shallow depth ($z_1 \in (0, 1.5)$) than more layers. However, for greater depths, a larger number of layers M' turns out to be more preferable. At $M' \geq 4$ the accuracy of the algorithm saturates. This is true for all observation layer heights considered.

Similar effects arose for the other considered lines of the composite source.

7 On the uniqueness of solution to the inverse problem

In discussing solutions to inverse problems, specific sets on which these solutions are sought are often not explicitly indicated. Nevertheless, words are spoken about the uniqueness or non-uniqueness of the solution. Meanwhile, the words like "an equation has a non-unique solution" have a certain meaning only after specifying the set on which the inverse problem should be solved. If this is not done, then it is implic-

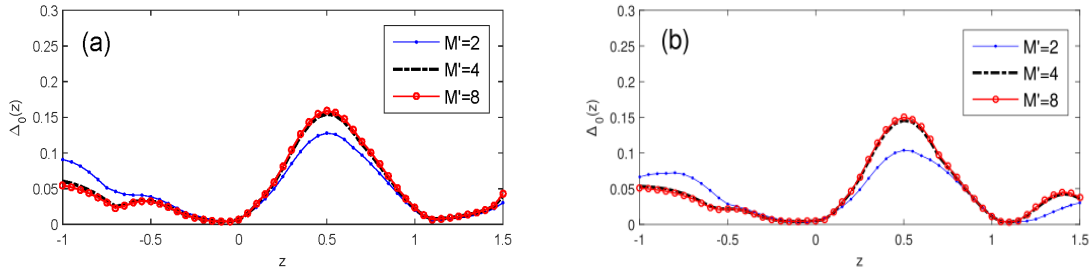

Figure 13: Composite source on ℓ_4. (a) Comparison of the accuracy of the $\Delta_0(z)$ algorithm for $z_3 = 2$ and for different numbers M' of sensor layers. (b) The same for $z_3 = 4$.

itly assumed that the corresponding set is the domain for the operator of the direct problem in postulated solution space. Selecting a single solution from their many requires introducing additional assumptions. These assumptions (constraints) can be of various natures. For example, they can be expressed by special inequalities for the solution and/or its functionals, they can be represented by properties such as source representability of solutions, etc. Constraints of this type must be determined by the user of solving algorithm and follow from the physical nature of solutions. However, in practice such constraints are often absent. Experience in solving numerous inverse problems shows that then it is convenient to use methods that allow us to search for special solutions with postulated optimal mathematical properties (see [1, 2, 11, 20, 25], etc.). So, these properties form a set of solutions, and sometimes this set consists of a single element. Let us illustrate how this is done in our approach.

At step 1 of Algorithm 2, the Fredholm integral equation should be solved that may not have a unique solution in the spaces indicated there. To eliminate this ambiguity, one can use such well-known procedures for solving inverse problems as A.N. Tikhonov's regularization method [25] or the TSVD method [11] with the choice of the appropriate regularization parameter based, for example, on the discrepancy principle [21]. The mentioned methods allow to find stably an approximation to the normal solution in L_2 of the equation (9), i.e. the solution with the minimal norm. Such a normal solution is always unique, and thus Algorithm 2 provides a unique solution to the inverse problem posed above.

In addition, procedures for finding a normal solution to the inverse problem can sometimes be adapted to the numerical study of the uniqueness in selected solution space. This is based on the following theoretical fragment.

For simplicity, let Z, U be Hilbert spaces and $A : Z \to U$ be a bounded linear operator. Consider the operator equation $Az = u$ and assume that for a given right-hand side $u \in U$, $u \neq 0$, it is solvable in the space Z. Then, as is known, the extremum problem of finding a normal solution, i.e. find an element $\bar{z} \in Z$ such that

$$\|\bar{z}\| = \inf \{\|z\| : \|Az - u\| = 0\}$$

has a unique solution $\bar{z} \neq 0$. Similarly, extremum problems of finding normal solutions $\tilde{z}(z_0) \in Z$ with respect to elements $z_0 \in Z$, i.e. tasks

$$\|\tilde{z}(z_0) - z_0\| = \inf \{\|z - z_0\| : \|Az - u\| = 0\}, \tag{13}$$

have a unique solution for every $z_0 \in Z$.

Proposition 1. If for any $z_0 \notin \ker A$ the equality $\tilde{z}(z_0) = \bar{z}$ holds, then $\ker A = 0$.

Proof. Suppose the proposition is not true. Then for any $z_0 \notin \ker A$ the equality $\tilde{z}(z_0) = \bar{z}$ is satisfied, but $\ker A \neq 0$. Take an arbitrary element $w \in \ker A$, $w \neq 0$. From (13) and the proposition condition it follows: $\|\tilde{z}(z_0) - z_0\| = \|\bar{z} - z_0\| < \|z - z_0\|$, $\forall z \neq \bar{z}$, $\forall z_0 \in Z$. In particular, for the elements $z = \bar{z} + w/2$, $z_0 = \bar{z} + w$ we obtain:

$$\|\bar{z} - z_0\| = \|w\| < \|z - z_0\| = \|\bar{z} + w/2 - (\bar{z} + w)\| = \|w/2\| \;\Rightarrow\; w = 0,$$

that contradicts the assumption $w \neq 0$.□

Corollary 1. If $\ker A \neq 0$, then there is an element $z_0 \notin \ker A$ such that $\tilde{z}(z_0) \neq \bar{z}$.

Let now the right side of the equation $Az = u$ be given with an error, namely, the element $u_\delta \in U$ is known such that $\|u - u_\delta\| \leq \delta$. Suppose that two families of stable approximations have been constructed for finding normal solutions: $\tilde{z}_\delta(z_0) \to \tilde{z}(z_0)$, $\bar{z}_\delta \to \bar{z}$ $(\delta \to 0)$.

Proposition 2. If $\|\tilde{z}_\delta(z_0) - \bar{z}_\delta\| \to 0$ for any $z_0 \notin \ker A$ as $\delta \to 0$, then $\ker A = 0$.

Indeed, if $\|\tilde{z}_\delta(z_0) - \bar{z}_\delta\| \to 0$ for $\delta \to 0$, then $\|\tilde{z}(z_0) - \bar{z}\| = 0$ for any $z_0 \notin \ker A$. Then, by Proposition 1, $\ker A = 0$. □

Corollary 2. If $\ker A \neq 0$, then there is an element $z_0 \notin \ker A$ such that $\|\tilde{z}_{\delta_n}(z_0) - \bar{z}_{\delta_n}\| \geq \text{const} > 0$ for at least one sequence $\delta_n \to 0$.

This corollary can be used to a certain extent in a numerical study on the non-uniqueness of solution to our inverse problem in L_2. Schematically, this is represented by the following procedure.

Let us consider a model problem for the equation (9), written in operator form $Az = u$, and having some given solution $\bar{z} \in Z$, $\bar{z} \neq 0$. Then we can calculate the corresponding right-hand side of this equation, $\bar{u} = A\bar{z}$, and find several of its perturbed realizations $u_\delta \in U$ with perturbation level $\delta > 0$, close to the rounding errors on the computer used. Then, for approximate inverse problems $Az = u_\delta$, it is possible to find normal solutions $\bar{z}_\delta$, using, for example, Tikhonov regularization. Similar regularized normal solutions $\tilde{z}_\delta(z_0) \in Z$ can be calculated with respect to various elements $z_0 \in Z$, $Az_0 \neq 0$. If we managed to find an element z_0 for which the inequality

$$\|\tilde{z}_\delta(z_0) - \bar{z}_\delta\| \geq C_0 = \text{const} > 0 \tag{14}$$

holds, with a constant C_0 significantly exceeding the rounding errors, then, taking into account Corollary 2, *there is reason to assume* that $\ker A \neq 0$, i.e. that the equation $Az = u$ does not have a unique solution in the space Z.

8 Numerical study of uniqueness

Such a non-uniqueness study for our inverse problem of acoustic sounding was carried out on the same model problem with a composite source lying on the line ℓ_4. Specifically, step 1 of Algorithm 2 was considered. Then, for each Ω, the normal solution $\tilde{V}_{norm}(z', \Omega; \tilde{V}_0) \in L_2[z_1, z_2]$ of the integral equation from (9),

$$\int_{z_1}^{z_2} \tilde{G}(z - z', \Omega)\tilde{V}(z', \Omega)dz' = \tilde{W}(z, \Omega), \quad z \in [z_3, z_4],$$

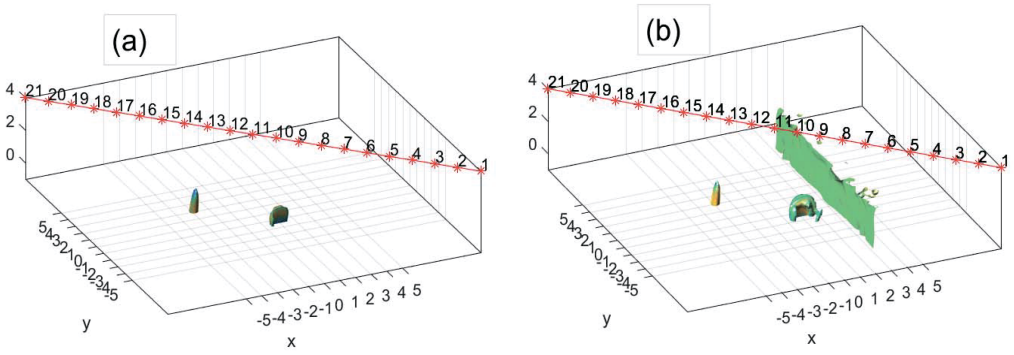

Figure 14: Numerical study of uniqueness. Images of approximate solutions $\xi_m(x)$ for different $z_0 = \tilde{V}_{0m}(z, \Omega)$: (a) $\xi_3(x)$; (b) $\xi_1(x)$.

was approximately calculated with respect to various elements $\tilde{V}_0(z', \Omega) \in L_2[z_1, z_2]$ using Tikhonov's regularization. In numerical experiments, these elements were taken as Fourier images $\tilde{V}_{0m}(z, \Omega) = F_{xy}[v_{0m}(x, y, z)](\Omega)$, $z \in [z_1, z_2]$, $(m = 0, 1, 2, 3)$ of functions

$$v_{00}(x, y, z) = 0,\ v_{01}(x, y, z) = 10^{-4}x,\ v_{02}(x, y, z) = 10^{-5}(x^2 + y^2 + z^2),$$
$$v_{03}(x, y, z) = 10^{-5}(x^2 - y^2 + z^2).$$

The result was a family of Tikhonov approximations $\tilde{V}_{tikh}(z, \Omega; \tilde{V}_{0m}) \in L_2[z_1, z_2]$. Therefore, in the notation from Section 7, the role of z_0 here is played by the quantities $\tilde{V}_{0m}(z, \Omega)$, $m = 0, ..., 3$, depending on the parameter Ω. The quantity $\bar{z}_\delta$ is presented by elements $\tilde{V}_{tikh}(z, \Omega; \tilde{V}_{00})$, and the values $\tilde{z}_\delta(z_0)$ correspond to approximate solutions $\tilde{V}_{tikh}(z, \Omega; \tilde{V}_{0m})$, $m = 1, 2, 3$. The left side of the inequality (14), used in analyzing the ambiguity of the solution of integral equations (9), can be written in relative form as

$$D_m = \frac{\left\| \tilde{V}_{tikh}(z, \Omega; \tilde{V}_{0m}) - \tilde{V}_{tikh}(z, \Omega; \tilde{V}_{00}) \right\|_{L_2[z_1, z_2]}}{\left\| \tilde{V}_{tikh}(z, \Omega; \tilde{V}_{00}) \right\|_{L_2[z_1, z_2]}},\ m = 1, 2, 3.$$

In our calculations, it turned out that $D_1 \approx 2.556$, $D_2 \approx 2.119$, $D_3 \approx 0.997$, and this, according to the theory from Section 7, serves as some basis for the conclusion about non-uniqueness of solutions to equations (9) in L_2.

Further applying Algorithm 2 for found functions $\tilde{V}_{tikh}(z, \Omega; \tilde{V}_{0m})$, $m = 1, 2, 3$, we can compare the corresponding approximate solutions $\xi_m(x)$ of our inverse problem with a solution for $m = 0$. An example of such a comparison is given in Fig.14, and it confirms the significant difference in the approximate solutions of the inverse problem for different m.

9 Conclusions

Previously, in the works [3, 4, 5] it was shown that Algorithm 2 for solving the three-dimensional inverse problem of acoustic sounding is very efficient in terms of solution

time. At the same time, as established in the above study, the accuracy of the resulting approximate solution depends significantly on the tuning of geometric parameters of the data recording system.

Firstly, this accuracy depends on the location of the point or composite source that excites oscillations in the system. Calculations have shown that the line of sources (such as lines $\ell_1 - \ell_4$), on the one hand, should not be far from the area of acoustic inhomogeneity, and on the other hand, point sources should be at some small angle to this areas.

Secondly, the accuracy of the resulting solution is affected by the height of the observation layer containing sensors for data recording. With an increase in this height, i.e. when the observation layer moves away from inhomogeneities, the accuracy improves at first for all source positions, but then remains virtually unchanged.

Thirdly, good accuracy of the approximate solutions is ensured even for a thin layer of data observation, that is, already for two planes of sensor location, and when the number of layers is greater than four, the accuracy of the algorithm stabilizes (saturates).

Finally, Algorithm 2 can, to a certain extent, be applied to numerically study of the ambiguity of solution to the inverse problem under consideration using the method from Section 7.

Acknowledgement

The work was carried out with the financial support of the Russian Science Foundation, project no. 22-71-10070

References

[1] Bakushinsky A., Goncharsky A., *Ill-Posed Problems: Theory and Applications.* Kluwer Academic Publishers, Dordrecht, 1994.

[2] Bakushinsky A.B., Kokurin M.Yu., *Iterative methods for approximate solution of inverse problems.* Mathematics and Its Applications, Kluwer Academic Publishers, Dordrecht, 2004.

[3] Bakushinsky A.B., Leonov A.S., *Fast numerical method of solving 3D coefficient inverse problem for wave equation with integral data.* J. of Inverse and Ill-Posed Problems. 26 (2018), no. 4, 477—492.

[4] Bakushinskii A.B., Leonov A.S., *Numerical solution of an inverse multifrequency problem in scalar acoustics.* Comput. Math. and Math. Phys. 60 (2020), no. 6, 987—999.

[5] Bakushinsky A.B., Leonov A.S., *Fast Solution Algorithm for a Three-Dimensional Inverse Multifrequency Problem of Scalar Acoustics with Data in a Cylindrical Domain.* Comput. Math. and Math. Phys. 62 (2022), no. 2, 287–301.

[6] Beilina L., Klibanov M.V., *Approximate Global Convergence and Adaptivity for Coefficient Inverse Problems.* Springer, New York, 2012.

[7] Belishev M.I., *Recent progress in the boundary control method.* Inverse Problems, 23 (2007), no. 5, 1—67.

[8] Burov V.A., Alekseenko N.V., Rumyantseva O.D., *Multifrequency generalization of the Novikov algorithm for the two-dimensional inverse scattering problem.* Acoust. Phys. 55 (2009), no. 6, 843—856.

[9] Burov V.A., Vecherin S.N., Morozov S.A., Rumyantseva O.D. *Modeling of the exact solution of the inverse scattering problem by functional methods.* Acoust. Phys. 56 (2010). no. 4, 541—559.

[10] Colton D., Kress R., *Inverse Acoustic and Electromagnetic Scattering Theory.* 2nd ed. Appl. Math. Sci. 93, Springer, Berlin, 1998.

[11] Engl H.W., Hanke M., Neubauer A., *Regularization of Inverse Problems.* Kluwer Academic Publishers, Dordrecht, 1996.

[12] Evstigneev R.O., Medvedik M.Yu., Smirnov Yu.G., Tsupak A.A., *Inverse problem of reconstructing body inhomogeneities for early disease detection by microwave tomographic imaging.* Izv. Vyssh. Uchebn. Zaved. Povolzh. Reg. Fiz.-Mat. Nauki. 44 (2017), no. 4, 3—17.

[13] Goncharskii A.V., Romanov S.Yu., *Two approaches to the solution of coefficient inverse problems for wave equations.* Comput. Math. Math. Phys. 52 (2012), no. 2, 245—251.

[14] Goncharskii A.V., Romanov S.Yu., *Supercomputer technologies in inverse problems of ultrasound tomography.* Inverse Problems. 29 (2013), no. 7, Article ID 075004.

[15] Goryunov M.A., Saskovets A.V., *Inverse Scattering Problems in Acoustics.* Mosk. Gos. Univ., Moscow, 1989 (in Russian).

[16] Kabanikhin S.I., Satybaev A.D., Shishlenin M.A., *Direct Methods of Solving Multidimensional Inverse Hyperbolic Problems.* VSP, Utrecht, 2004.

[17] Klibanov M.V., Kolesov A.E., *Convexification of a 3-D coefficient inverse scattering problem.* Computers and Mathematics with Applications. 77 2019, no. 6, 1681—1702.

[18] Klibanov M.V., Kolesov A.E., Dinh-Liem Nguyen. *Convexification method for an inverse scattering problem and its performance for experimental backscatter data for buried targets.* SIAM J. Imaging Sciences. 12 2019, no. 1, 576—603.

[19] Klibanov M.V., Jingzhi Li, *Inverse Problems and Carleman Estimates. Global Uniqueness, Global Convergence and Experimental Data.* De Gruyter, Berlin/Boston, 2021.

[20] Leonov A.S., *Solution of Ill-Posed Inverse Problems: Theory, Practical Algorithms, and Demonstrations in MATLAB.* Librokom, Moscow, 2013 (in Russian).

[21] Morozov V. A., *Methods for Solving Incorrectly Posed Problems.* Springer-Verlag, New York, 1984.

[22] Novikov R.G., *Reconstruction of a two-dimensional Schrodinger operator from the scattering amplitude for fixed energy.* Funct. Anal. Appl. 20 (1986), no. 3, 246—248.

[23] Pestov L.N., Bolgova V.M., Danilin A.N., *Numerical reconstruction of three-dimensional speed of sound by applying a boundary control method.* Vestn. Yugor. Gos. Univ. (2011), no. 3, 92—98.

[24] Ramm A.G. *Multidimensional Inverse Scattering Problems.* Pitman Monogr. Surv. Pure Appl. Math. 51. Longman Scientific and Technical, Harlow, 1992.

[25] Tikhonov A.N., Goncharsky A.V., Stepanov V.V., Yagola A.G., *Numerical Methods for the Solution of Ill-Posed Problems.* Nauka, Moscow, 1990; Kluwer Academic, Dordrecht, 1995.

A.B. Bakushinsky
Institute for Systems Analysis,
Federal Research Center “Computer Science and Control”,
Russian Academy of Sciences
Moscow, 117312 Russia
Mari State University, Yoshkar-Ola,
424000 Mari El Republic, Russia
E-mail: bakush@isa.ru,

A.S. Leonov
Department of Higher Mathematics
National Research Nuclear University “MEPhI”
Moscow, 115409 Russia
E-mail: asleonov@mephi.ru

Received 10.02.2024, revised 04.03.2024, Accepted 05.03.2024